

# Laboratory Capacity Modulation Experiments, Analyses, and Validation\*

*W. A. Miller*

Oak Ridge National Laboratory  
Oak Ridge, TN 37831

## Abstract

A combined experimental and analytical project was conducted on a breadboarded continuously variable speed air-to-air heat pump (CVSHP). The split-system residential unit of nominal 2 3/4-ton (9.7-kW) cooling capacity was instrumented and tested in environmental chambers. The steady-state, frosting/demand defrosting, and cycling efficiency characteristics of the CVSHP with first generation components (e.g., heat exchangers, compressor, and indoor blower, both having variable speed induction motors) were measured in the laboratory for compressor drive frequencies ranging from 15 through 90 Hz. Steady-state efficiency data were used to validate an initial version of the Oak Ridge National Laboratory steady-state modulating heat pump design program. Algorithms were developed from reduced dynamic loss data from which calculations were made of the seasonal losses for the test CVSHP.

## Introduction

A planned series of experiments were conducted to characterize the efficiency and efficiency trends of a continuously variable speed heat pump (CVSHP). The primary objectives of this study were to determine the efficiency of a CVSHP at different speeds and ambients, to identify the effect of dynamic losses, to develop control strategies to reduce the dynamic losses, and to perform seasonal analyses to assess the benefits of the CVSHP technology as applied to the particular system tested. Steady-state test data were also used to validate the Oak Ridge National Laboratory (ORNL) modulating heat pump computer code.

Calorimeter testing of advanced variable speed compressors and testing of state-of-the-art CVSHPs is planned.

## Summary of Work

A continuously variable speed, air-to-air split-system residential heat pump of nominal 2 3/4-ton (9.7-kW) cooling capacity was instrumented with temperature and pressure sensors, with locations displayed in Fig. 1. Testing was conducted in environmental chambers, which were capable of controlling indoor and outdoor ambient dry bulb and dew point temperatures. A host computer and data acquisition system were used to monitor all temperatures, pressures, powers, and flows. Salient features of both the breadboard CVSHP and the test stand are discussed in previous work by Miller.<sup>1</sup>

A series of tests were conducted on the test CVSHP in the laboratory to demonstrate optimal refrigerant flow and airflow control for best coefficient of performance (COP) as constrained by comfort. The capillary tubes originally supplied with the test unit were replaced with variable area, hand-controlled valves (Fig. 1) to improve control of refrigerant flow during testing. As seen in Fig. 1, the compressor was driven by a motor-generator (M-G) set (i.e., ideal induction motor drive), and the indoor blower was driven by a first generation inverter drive, which was originally supplied with the test unit.

The optimal flow control experiments were conducted in the heating mode at outdoor ambient temperatures of 40 and 10°F (4.4 and -12.2°C) and in the cooling mode at outdoor ambient temperatures of 95 and 82°F (35 and 27.2°C). Test parameters were compressor speed, indoor blower speed, and refrigerant subcooling at the condenser exit. A range of condenser exit subcoolings (controlled by the variable area throttling valve) and indoor airflows for compressor drive frequencies ranging from 15 to 90 Hz were tested to observe their effect on

\* Research sponsored by the Office of Buildings and Community Systems, U.S. Department of Energy, under Contract DE-AC05-84OR21400 with Martin Marietta Energy Systems, Inc.

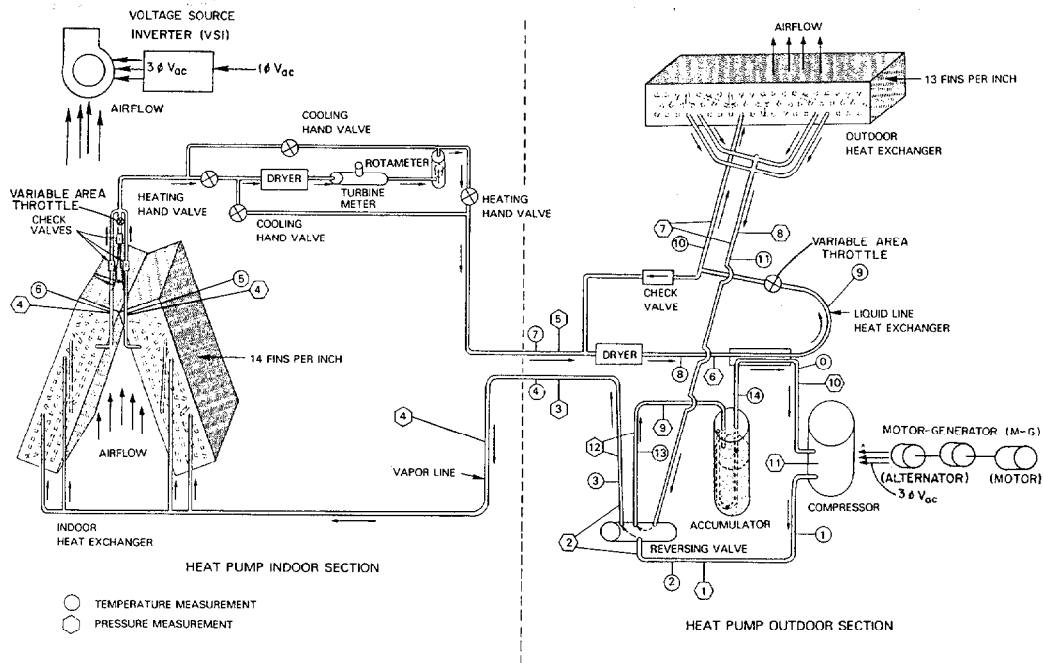


Fig. 1. Schematic and sensor locations for the tested continuously variable speed heat pump (CVSHP).

COP, capacity, and component efficiencies. From these tests, an optimal ratio of compressor motor speed to indoor blower speed and the optimal level of subcooling at condenser exit as a function of compressor speed were identified in the laboratory.

The data from the optimal flow control study and the calorimetry data, obtained from a compressor manufacturer on an identical reciprocating compressor as tested in the laboratory CVSHP, were both used to validate the initial version of the ORNL steady state modulating heat pump design model (MHPDM).<sup>2</sup>

The operating efficiencies of the first generation variable speed hermetic reciprocating compressor and indoor centrifugal blower, both having induction motors, were characterized while operating under optimal flow control conditions as determined from the experiments discussed above. The indoor blower was tested using a six-step voltage source inverter (VSI) designed in the late 1970s and also using an M-G set (ideal induction motor drive) for a motor drive frequency range of 20 to 60 Hz. The reciprocating compressor was driven in separate

tests by a VSI,<sup>a</sup> a pulse-width modulated inverter (PWMI),<sup>b</sup> and the M-G set to observe the effect of each adjustable-speed drive on the efficiency of the compressor for drive frequencies ranging from 15 to 90 Hz.

Follow-up laboratory work was conducted on the optimally controlled system to measure the COP and system capacity during frosting/demand defrosting tests and during both heating and cooling mode cycling tests. Frosting/demand defrosting tests were conducted for a range of compressor speeds, outdoor air temperatures, and relative humidities. Cycling tests were conducted for a range of compressor speeds and outdoor temperatures. Cycling rate was set at 12 min on and 48 min off as suggested by some heat pump manufacturers.<sup>3</sup> The dynamic loss testing was

a Commercially available in 1979 and supplied with the test unit.

b International product commercially available in 1983 and designed to have diminished harmonics and torque pulsation effects as compared with earlier design PWMI drives.

conducted while the CVSHP operated under previously determined optimal refrigerant flow and airflow control settings. Previous studies by Tanaka et al.<sup>4</sup> and by Miller,<sup>5</sup> dealing with cycling dynamics, and by Kuwahara et al.,<sup>6</sup> dealing with defrosting efficiency, and by Glamm,<sup>7</sup> dealing with dynamic control, were gleaned for techniques to minimize the dynamic losses of the test CVSHP. A best dynamic control strategy for the test system was developed in the laboratory and dynamic loss algorithms were developed from the data. Seasonal analysis simulations were then made using a binned seasonal performance computer code developed by Rice et al.<sup>8</sup> to estimate the energy savings directly attributable to (1) the reduction of dynamic losses for single-speed heat pumps (SSHPs), and (2) the efficiency improvement due to compressor and indoor blower speed modulation.

#### Technical Accomplishments

##### CVSHP Optimal Flow Control - Laboratory Demonstration

Optimal levels of refrigerant subcooling at the condenser exit were identified at discrete compressor speeds during heating and cooling mode laboratory tests. Refrigerant-side COP measurements observed in the heating mode at 40°F (4.4°C) outdoor temperature and in the cooling mode at 82°F (27.7°C) outdoor temperature are plotted in Figs. 2 and 3, respectively. Various families of refrigerant subcooling (at the condenser exit) per compressor speed tested are displayed as functions of indoor blower speed. The dashed curves in Figs. 2 and 3 are simulation results of the initial version of the ORNL steady state MHPDM. These curves are included for indication of model absolute and trend accuracy in predicting optimal COP and capacity performance of the test CVSHP.

**Heating mode.** Refrigerant subcooling of 5-10 F° (3-6 C°) was observed to yield optimal or near optimal COP for compressor speeds of 30 to 90 Hz operating in 40 and 10°F (4.4 and -12°C) outdoor air ambients. For these heating mode test results, the indoor blower (inverter driven) could actually be set at a constant 45-Hz speed with less than a 2% drop in COP measured at the optimum blower speed (Fig. 2).

Best COP measurements (Fig. 2) indicate approximately an 8% increase in COP when the compressor speed is lowered from 60 to 30 Hz. However, when the speed is lowered from 30 to 15 Hz, the measured COP dropped by 20%. This drop in COP at 15 Hz can be attributed to (1) a loss in heat exchanger efficiency and (2) a drop in

#### WITH OPTIMAL CONTROL, EFFICIENCY INCREASES DOWN TO 30-Hz COMPRESSOR SPEED

- Heating mode steady-state tests
- Outdoor air temperature 40°F
- Indoor air temperature 70°F

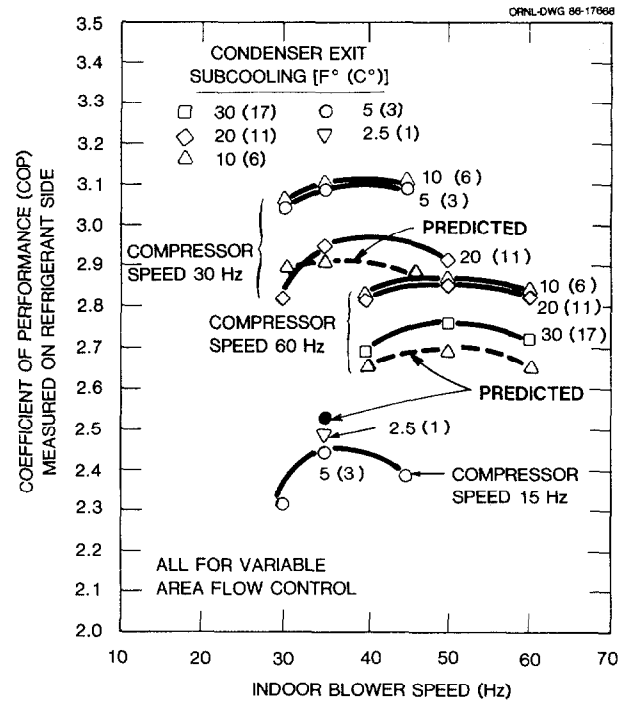


Fig. 2. Measured and predicted heating mode COP for the variable speed heat pump operating at 40°F (4.4°C) outdoor air temperature.

the isentropic efficiency<sup>c</sup> of the compressor, as explained in previous work by Miller.<sup>9</sup> It should be noted that testing at 55°F (12.7°C) outdoor temperature (not shown in Fig. 2) did not show a drop in COP, as compressor speed was reduced from 30- to 15-Hz compressor drive frequency. The refrigerant mass flow rate was greater at 55°F (12.7°C) outdoor temperature than at 40°F (4.4°C), and the pressure ratio across the compressor was reduced. Therefore both compressor and heat exchanger efficiencies were improved, resulting in improvement of COP trends as speed decreased at the 55°F (12.7°C) outdoor ambient.

<sup>c</sup> Compressor isentropic efficiency is defined here as the ratio of isentropic compressor work (computed across the shell) to the measured power input.

**OPTIMAL LEVEL OF REFRIGERANT SUBCOOLING DECREASES WITH REDUCTION IN COMPRESSOR SPEED**

- Cooling mode steady-state tests
- ARI ambient air test conditions
  - Outdoor air temperature 82°F
  - Indoor dry bulb 80°F; wet bulb 67°F

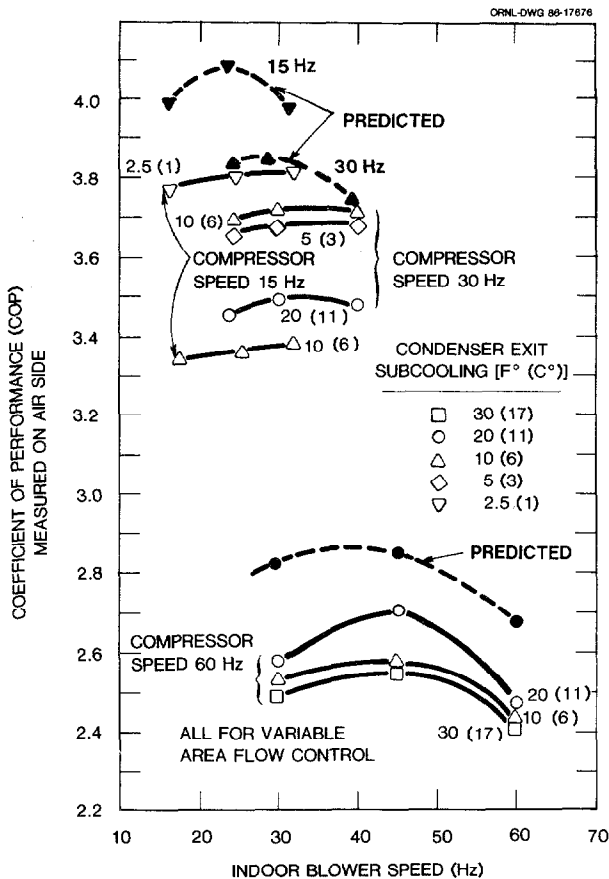


Fig. 3. Cooling mode COP measurements and predictions made at 82°F (27.7°C) outdoor air temperature.

Cooling mode. Best COPs in cooling mode required a greater change in blower speed and refrigerant subcooling with change in compressor speed. The indoor blower speed varied from 45 Hz at a compressor drive frequency of 60 to 16.7 Hz at compressor drive frequency of 15 Hz, as indicated in Fig. 3. Refrigerant subcooling for optimal COP at 60-Hz compressor speed and 82 and 95°F (27.7 and 35°C) outdoor air temperature was 20 F° (11 C°), while at 45- through 15-Hz compressor speed, optimal subcooling varied from 20 to 2.5 F° (11 to 1.4 C°).

Reducing the compressor drive frequency from 60 to 30 to 15 Hz at the 82°F (27.7°C) outdoor ambient<sup>d</sup> resulted in an improvement in COP

<sup>d</sup> Near the expected minimum speed balance point in cooling mode.

(Fig. 3), a trend not previously observed in heating mode testing at 40°F (4.4°C).<sup>e</sup> At 15-Hz compressor drive frequency, the cooling mode refrigerant mass flowrate, measured at 82°F (27.7°C), was double the heating mode mass flowrate, measured at 40°F (4.4°C), because of the higher operating evaporator temperature. Thus, apparently there was no reduction in refrigerant-side heat flux in cooling mode as compared to heating mode, when operating at 15-Hz compressor drive frequency.

CVSHP Optimal Flow Control - Model Validation

The initial version of the MHPDM, based on the single-speed model developed by Rice and Fischer,<sup>10</sup> was validated against optimal flow control test data of the CVSHP. The model matched the measured trends of COP and capacity very well, slightly underpredicting heating COP and capacity and overpredicting cooling COP and capacity (COP predictions illustrated in Figs. 2 and 3). Prediction agreement was best at low-speed conditions for both heating and cooling. The poorest agreement occurred at the 95°F (35°C) nominal speed (60 Hz) rating condition where predictions were 10% greater than measured data. The overprediction in cooling at higher speeds was due to the inaccuracy of the simplified heat exchanger submodels when simulating complex circuitry under high levels of refrigerant subcooling at condenser exit. The validation results indicated that the model was well suited for use in evaluating design and operating options, provided that the heat exchangers were efficiently circuited and operated with low to moderate [ $<20$  F° (11 C°)] condenser subcooling and low evaporator superheat. Outside these situations, the use of tube-by-tube heat exchanger models may be required.

Demonstrated Refrigerant Charge Variation for CVSHP

Testing was conducted to determine the optimal refrigerant charge required for both low superheat at the inlet to the compressor and optimal level of refrigerant subcooling at condenser exit. Results displayed in Fig. 4 indicated optimal refrigerant charges varied by roughly 1.5 lbs (0.6 kg) over the range of compressor speeds tested in cooling and heating modes, except for heating mode operation at 15-Hz compressor speed. Here 11.5 lb (5.2 kg) of refrigerant was required to duplicate optimal system efficiency, 2.5 lb (1.1 kg) more refrigerant than required in cooling mode operation.

<sup>e</sup> Near the expected minimum speed balance point in the heating mode.

**OPTIMAL REFRIGERANT CHARGE INCREASES SIGNIFICANTLY ONLY AT 15-Hz HEATING**

- Manufacturer's nameplate charge 7.5 lb

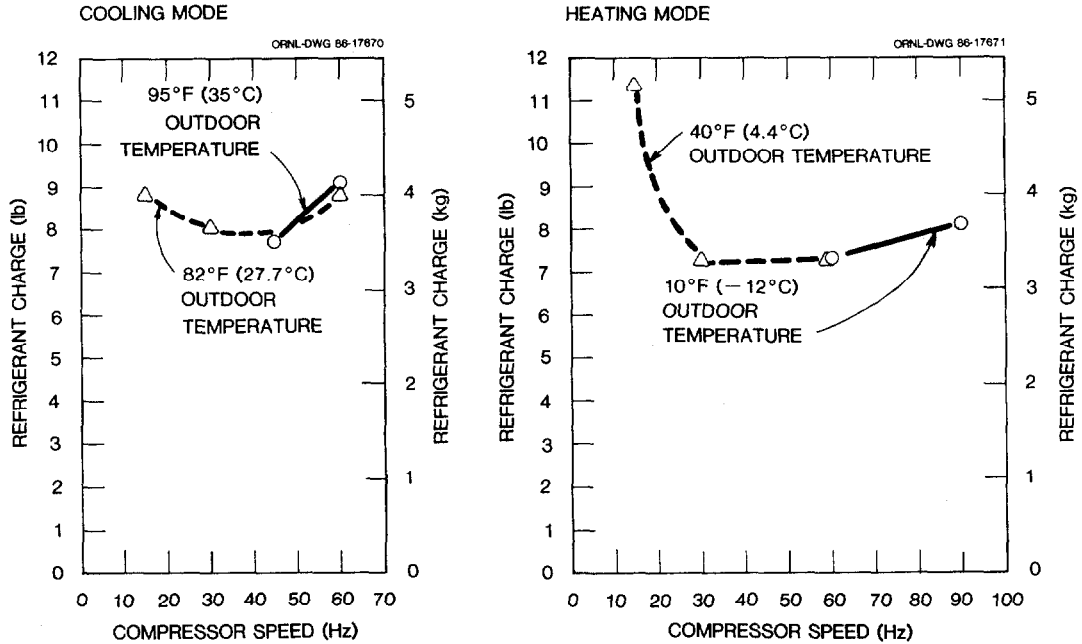


Fig. 4. Optimal refrigerant charge required for both low superheat at the inlet of the compressor and optimal level of refrigerant subcooling at the condenser exit.

This difference occurred because of the low refrigerant velocity in heating versus cooling mode (implied from mass flowrate comparison), which resulted in a less efficient condenser heat transfer in heating mode, as discussed by Miller.<sup>9</sup>

Proved CVSHP Would Maintain Comfort

Laboratory work demonstrated that the CVSHP would maintain comfort at least as well as a single-speed heat pump under most conditions. Comparison of the CVSHP performance, having optimal airflow and refrigerant flow control settings, to a manufacturer's data for a single-speed heat pump (SSHP) indicated that the CVSHP satisfied both heating and cooling comfort requirements, while better following house load through capacity modulation.

Heating comfort. Capacity and delivery air temperature for an SSHP are listed in Table 1, with similar data for the optimal COP operating points of the CVSHP. Comfort is maintained with the CVSHP operating at 30-Hz compressor speed, and the part-load capacity would better match house load as compared with a single-speed unit. At the lower temperature of 10°F (-12°C) and 90-Hz compressor speed, the CVSHP had a measured

**TABLE 1**  
Capacity and supply air temperature for a single-speed heat pump and the continuously variable speed heat pump

Outdoor temperature (°F)	Heat pump type	Capacity (kBtu/h)	Supply air (°F)	Compressor speed (Hz)
40	Single speed <sup>a</sup>	32.1	94.8	60
		17.0	92.4	30
	Variable speed	11.5	85.7	20
		8.5	81.6	15
		16.1	82.4	60
10	Single speed	16.1	82.4	60
	Variable speed	22.6	92.8	90
		17.3	86.7	60

<sup>a</sup>Manufacturer's data for a single-speed heat pump operating with a capillary tube flow control.

capacity of 22.6 kBtu/h (6.6 kW), while the SSHP had a capacity of 16.1 kBtu/h (4.7 kW). Delivery temperature for the CVSHP is 93°F (34°C), while for the single-speed unit (operating without supplemental heaters), the delivery temperature is only 82.4°F (28°C). By overspeeding the compressor, comfort is maintained below the balance point of the single-speed unit

with less added energy due to supplemental heat. These results indicate that the test unit, operating as a CVSHP with optimal blower speed and refrigerant subcooling satisfies comfort requirements as well as the single-speed unit does and better follows house load.

Cooling mode. Sensible heat ratios (SHRs) for the optimal test operating points of the CVSHP are plotted in Fig. 5, with manufacturer single-speed data. Also a SHR boundary line is displayed that represents the required latent load simulated for an 1800-ft<sup>2</sup> (167-m<sup>2</sup>) house in Knoxville, Tennessee. Optimal operating points tabulated and plotted in Fig. 5 indicate, in terms of SHR, the test heat pump to have adequate latent capacity for humidity control within a residence. The optimum operating points for the CVSHP unit have an SHR comparable to or lower than the single-speed unit for outdoor temperatures of 95 and 82°F (35 and 27.7°C).

#### CONTINUOUSLY VARIABLE SPEED HEAT PUMP MAINTAINS GOOD HUMIDITY CONTROL

- Sensible heat ratio (SHR)
  - Optimal CVSHP operating points
  - Manufacturer operating points (single speed)

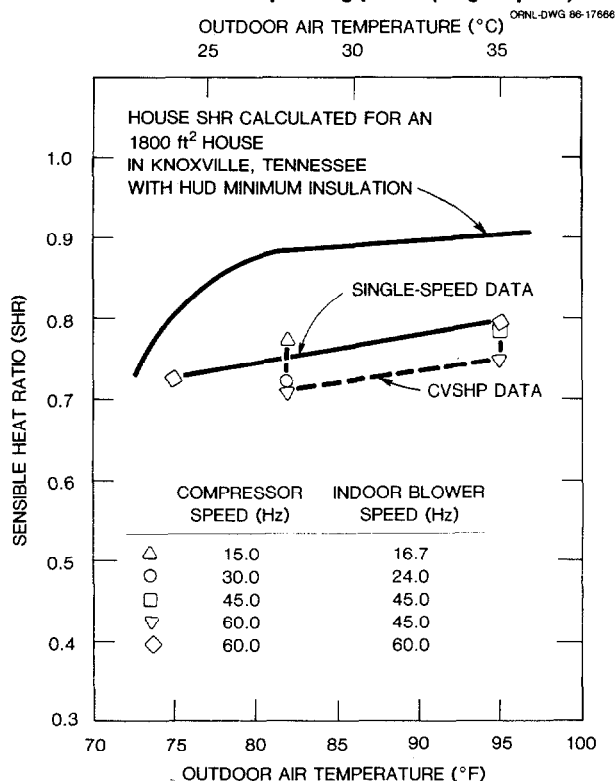


Fig. 5. The SHRs from manufacturer data for a single-speed heat pump (SSHP) compared to measured values for the optimal operating points of the continuously variable speed heat pump (CVSHP).

These results indicate that the CVSHP, having near equal total capacity at 60 Hz to the SSHP, has greater latent capacity and, thus, should provide a greater degree of comfort.

#### Characterized Efficiency Limits of First Generation Variable Speed Reciprocating Compressor

Laboratory data were used to characterize the effect of various adjustable speed drives on the overall isentropic efficiency of the test compressor. The compressor isentropic efficiency was measured during both heating and cooling mode optimal flow control tests and is plotted as a function of compressor drive frequency in Fig. 6. The lower curves in Fig. 6 represent the efficiency losses of the PWMI and the efficiency losses of the compressor and induction motor due to harmonics of the PWMI. The sum of the lower two curves in each cooling and heating mode plot therefore represents the combined compressor, motor, and drive efficiency losses.

Compressor and M-G drive. The compressor isentropic efficiency remained fairly constant from 60 to about 20 Hz (i.e., one-third nominal speed), with the compressor driven by the M-G set. At 15-Hz speed, the efficiency decreased 20% from the efficiency measured at 60 Hz. The rapid drop in efficiency for constant torque application below 20% speed was similar to results observed by Skogsholm,<sup>11</sup> and was partly due to an increase in the relative slip.

Compressor and PWMI drive. Efficiency trends with the PWMI drive were similar to those observed with the M-G drive; however, the losses in compressor isentropic efficiency due to the PWMI drive increased as speed decreased. In Fig. 6, results of testing at 60-Hz drive frequency and 40°F (21°C) outdoor temperature indicated that compressor efficiency, with the PWMI drive efficiency included, dropped 12% from that with the M-G drive. Roughly half of the efficiency degradation was due to efficiency losses in the PWMI (i.e., 5% loss), and the remainder was due to the effect of inverter harmonics on the compressor and motor as depicted by the efficiency loss curves in Fig. 6. Similar results were also observed in the cooling mode for tests conducted at 82°F (28°C) outdoor temperature and 60-Hz drive frequency.

At 15-Hz drive frequency, the compressor efficiency losses due to the PWMI drive increased to 25% in the heating mode and to 30% in the cooling mode. The efficiency losses from only the inverter ranged from 5% at 60 Hz, near full-rated load, to 7.5% at 15 Hz, and therefore did not nearly account for the total losses as speed was reduced (Fig. 6). The observed increase in efficiency losses was a result of the effect of current harmonics on the induction

**PULSE-WIDTH-MODULATED INVERTER (PWMI, 1984 DESIGN)  
LOSSES INCREASE AS COMPRESSOR SPEED DECREASES**

- TESTS CONDUCTED AT SAME OPERATING CONDITIONS  
PER COMPRESSOR SPEED

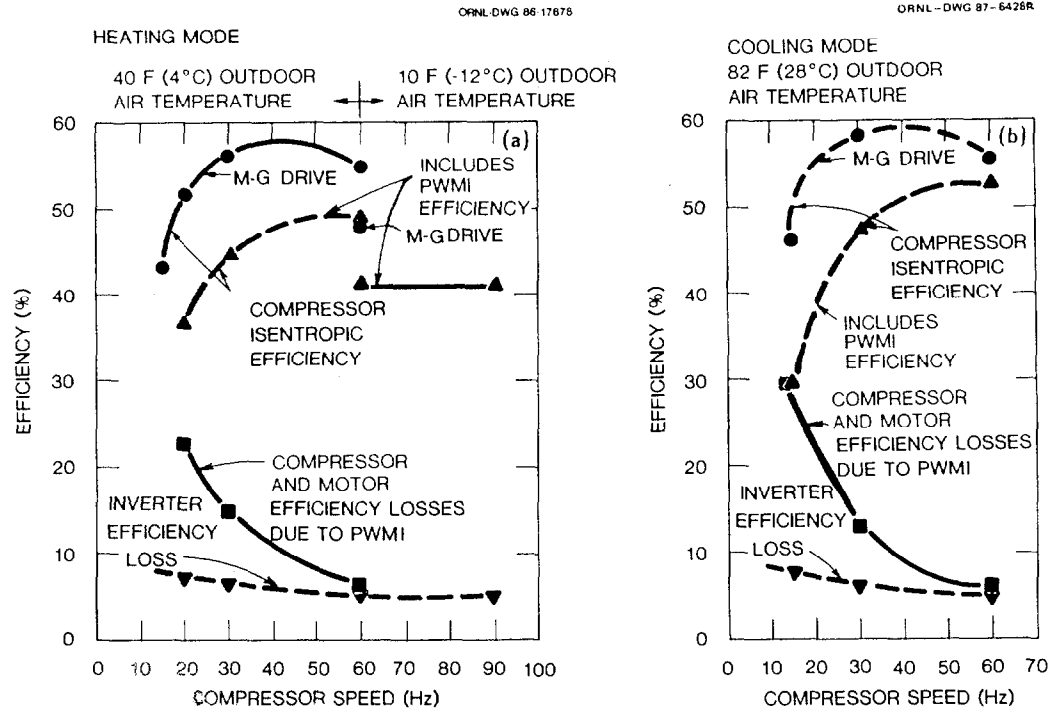


Fig. 6. Compressor isentropic efficiency and efficiency losses measured during steady state optimal flow control testing of the CVSHP.

motor of the compressor. Mohan<sup>12</sup> attributed the increase in induction motor losses due to inverter harmonics to be principally a result of increased stator and rotor winding losses and stray load losses.

These high-frequency harmonics of the PWMI can lead to excessive losses by imposing a series of high-voltage impulses on the motor windings. Andreas<sup>13</sup> stated that these high-frequency currents tend to be concentrated in areas of high flux density and to result in heat generation that increases motor winding temperature, which will in turn lead to additional suction gas superheating prior to compression. Jacobs<sup>14</sup> determined experimentally that as the amount of superheating increases, the effective compressor efficiency decreases [i.e., observed a 2% loss in compressor performance for every 10 F° (5.5 C°) rise in suction temperature]. Therefore, the harmonic content of the PWMI drive (a direct loss in motor efficiency) and the resultant additional suction gas superheating combine to result in the drop in

compressor isentropic efficiency shown in Fig. 6.

Compressor and VSI drive. Testing with the VSI drive caused a noticeable drop in compressor isentropic efficiency similar to that of the PWMI drive as compressor speed was reduced. At 60 Hz for both heating and cooling mode tests, the isentropic efficiency was 10% below that measured with the M-G drive. At 50% speed (i.e., 30-Hz speed) the compressor efficiency losses due to the VSI increased to 30% in heating mode and to 20% in cooling mode. Further lowering of the compressor speed to 15 Hz resulted in even larger efficiency losses of roughly 35%. The increase in compressor efficiency losses as speed is reduced is due to the effect of harmonics produced by the VSI drive. The VSI produced fairly high third, fifth, seventh, eleventh, and thirteenth harmonic currents for all modulation frequencies. These harmonics do not contribute to the output torque and result in increased motor losses and motor temperature, both of which decrease the compressor isentropic efficiency.

Characterized the Magnitude of Compressor Efficiency Losses Resulting from First Generation Inverter Drives

Compressor efficiency losses measured with specific models of both PWMI and VSI style inverters operating at nearly identical conditions are plotted in Fig. 7. It must be noted that this comparison should not be generalized due to the continuing advancement of both VSI and PWMI designs and the specific technologies of the components utilized. Also, the effect of harmonic currents would be different with a different motor design. Mohan<sup>12</sup> indicated that induction motors with high values of leakage reactance (i.e., leakage flux through airgap that leads magnetizing current by 90°) will have less harmonic currents and lower harmonic losses. With due regard for the above caveats, results in Fig. 7 show that in the cooling mode at near full load, the compressor efficiency losses due to the PWMI were similar to losses due to the VSI. In the heating mode, the PWMI caused roughly 30% less compressor efficiency losses for drive frequencies of 20 and 30 Hz. Compared with the results shown by Skogsholm<sup>11</sup> and Lloyd,<sup>15</sup> both of which compared PWMI with VSI, the micro-processor control of the PWMI voltage pulse rate reduced current harmonics and

improved PWMI efficiency to levels comparable to, if not better than, VSI designs of the late 1970s. The results shown here indicate the magnitude of losses to expect with these first generation drives. Rice<sup>16</sup> has shown that an advanced prototype variable speed motor and inverter drive (i.e., permanent magnet electronically commutated motor) would have a combined efficiency even higher than that of an induction motor with ideal induction motor drive (M-G set).

Characterized Efficiency Limits of First Generation Variable Speed Indoor Blower

Measured efficiency of the combined blower and blower motor when driven by the M-G drive with optimal voltage control was compared with measured efficiencies when the blower was driven by the VSI. The blower and drive system (motor and inverter) efficiency trends for the VSI drive and for an assumed 100% efficient VSI drive were calculated using measured single-phase input and three-phase output power, respectively (Fig. 8). The combined blower and blower motor efficiency for the 100% efficient VSI was only 5% less than that measured with the blower driven by the M-G set with optimal voltage control. This small difference indicates

- TESTED PWMI EFFICIENCY COMPARABLE TO TESTED VSI NOT GENERALIZED FOR ALL INVERTERS
- ADVANCEMENT OF DESIGNS
- MOTOR DESIGN

ORNL-DWG 87-6496

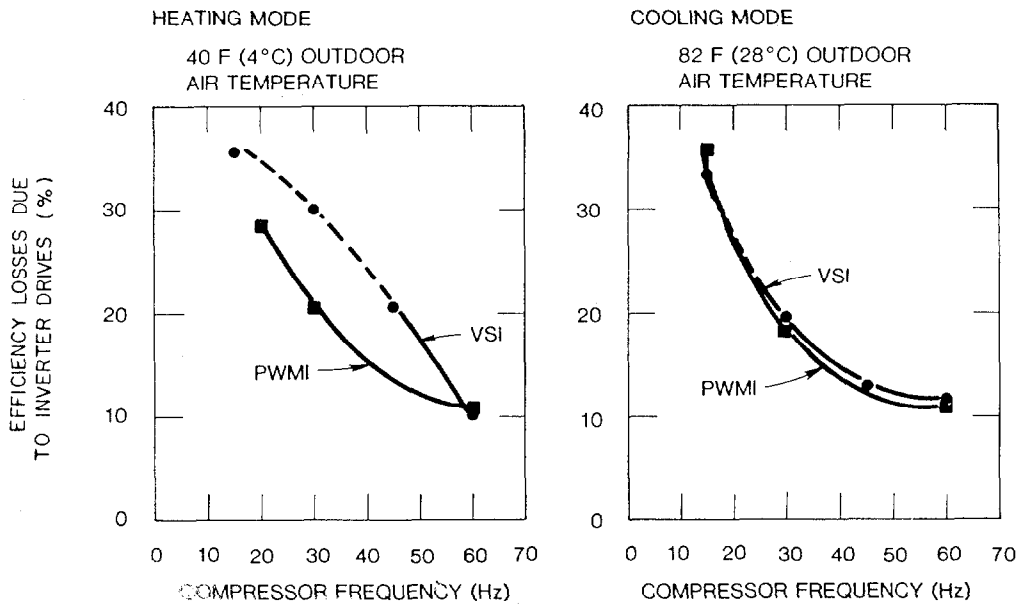


Fig. 7. Combined compressor, compressor motor and inverter efficiency losses for first generation inverter drives.

- VSI DRIVE INEFFICIENCY SIGNIFICANTLY DROPS COMBINED BLOWER AND BLOWER MOTOR EFFICIENCY
- OPTIMUM-SPEED CONTROL FOR BLOWER DRIVEN BY M-G DRIVE

ORNL-DWG 87-6431R

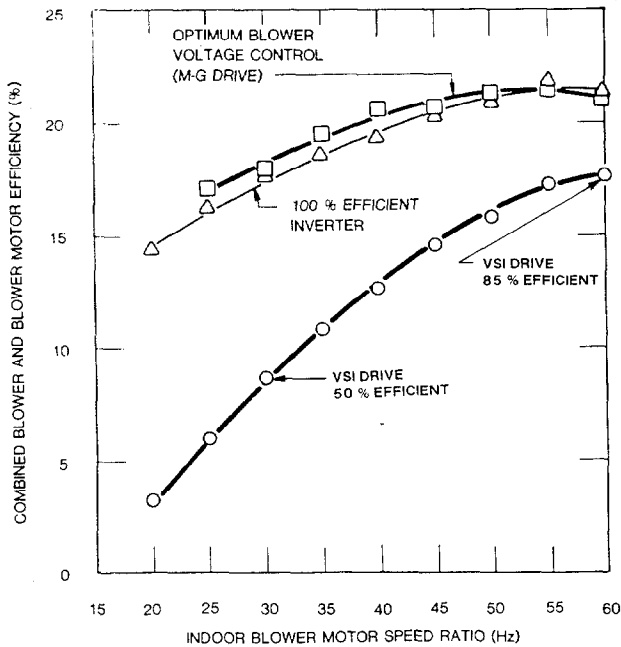


Fig. 8. Combined blower and blower motor efficiencies observed for VSI drive and M-G drive, both having optimal voltage control.

that the choppy waveform of the VSI had little effect on blower motor efficiency because the power measurement included inverter harmonics.

Similar trends for another VSI-inverter-driven and sine-wave-driven induction motor were observed by a motor/control manufacturer as reported by Rice.<sup>16</sup> In the data shown by Rice,<sup>16</sup> the efficiency of a three-phase, 1/3-hp (0.25-kW) induction motor (driven by M-G) dropped from 75% at full speed (1075 rpm) to 40% at one-third of full speed (400 rpm). The drop in motor efficiency was caused by the fixed losses of the stator core becoming a larger percentage of the total losses at reduced power output (i.e., power reduces roughly by the cube of the speed). Motor slip has little effect on efficiency as speed drops, because the torque drops as the speed squared and therefore the relative slip does not increase as in a constant torque application.

The combined blower and VSI drive system efficiency dropped sharply compared with efficiency observed for the M-G driven motor with optimal voltage control. At 60-Hz drive frequency, the VSI was measured to be 85% efficient. The VSI inefficiency and VSI harmonics

caused the efficiency at 60 Hz to be 16% less than that measured with the blower driven by the optimally controlled M-G set. Decreasing the blower speed to 20 Hz caused these losses to increase (Fig. 8) resulting in roughly a 77% drop in combined blower and blower motor efficiency compared with that of the M-G set.

#### Characterized the Frosting Dynamics of the CVSHP

Tests conducted at 35, 25, and 17°F (1.7, -3.9, and -8.3°C) outdoor temperature and 80% relative humidity revealed slight degradation in COP and heating capacity due to frosting of the outdoor coil. The density of refrigerant entering the compressor remained fairly constant over time for each test; as a result the evaporator capacity did not drop appreciably. The near constant refrigerant density caused the refrigerant mass flowrate and compressor power to be only slightly affected by frosting of the outdoor coil. Therefore, only marginal drops in COP and capacity were observed despite the accumulation of frost on the slanted outdoor heat exchanger, which had 13 wavy fins per inch. The defrost interval, defined as the time between defrosts, is carpet plotted in Fig. 9 as a function of both compressor drive frequency and outdoor temperature for a relative humidity of 70%. An operating line for simulated CVSHP operation in Nashville, Tennessee, is also shown in Fig. 9.

The operating line in Fig. 9 shows that a minimum defrost interval occurs at 60-Hz drive frequency and 21°F (-6.1°C) outdoor air temperature. Reducing the compressor speed along the operating line increases the defrost interval due to the increase in evaporator temperature as speed decreases. Overspeeding above 60 Hz operation in Nashville would occur at outdoor temperatures less than 21°F (-6.1°C). Therefore defrost intervals increase because the ambient air holds very little moisture.

Each frosting test was followed by an automatically initiated demand defrost based on outdoor coil air pressure drop. Visual observations indicated that the outdoor coil was heavily frosted at the start of each defrost. As seen in Fig. 9, reducing the outdoor temperature and/or the compressor drive frequency caused significant increases in the time to defrost initiation. Figure 9 indicates that no frosting of the outdoor coil would occur at 15°F (-9.4°C) or less with the compressor driven at modulation frequencies less than 60 Hz.

#### Characterized CVSHP Demand Defrosting Dynamics and Improved Defrosting Efficiency

Tests were conducted where the compressor drive frequency was increased to 90 Hz and/or the indoor variable area throttle was controlled

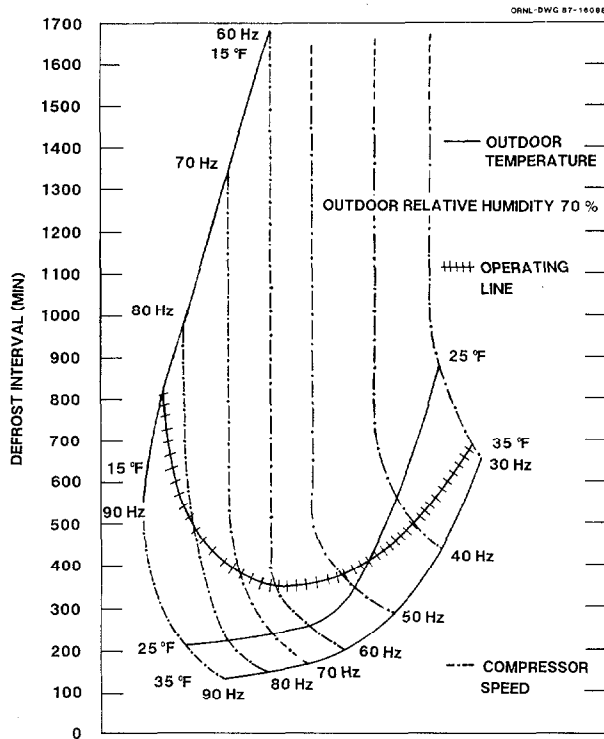


Fig. 9. Defrost intervals as a function of compressor drive frequency and outdoor air temperature with relative humidity held constant at 70%. Operating line is for simulated CVSHP operation in Nashville, Tennessee.

to determine any improvement in defrost efficiency due to these actions. Defrost data and test results are listed in Table 2. Data in Table 2 are from defrost tests that immediately followed frosting tests conducted at 60-Hz compressor speed and 35°F (1.7°C) temperature.

**TABLE 2**  
Defrost efficiency as affected by flow area of the indoor throttle and compressor overspeeding

Laboratory data	Compressor frost/defrost speed (Hz)			
	60/60		60/90	
Effective throttle area (in. <sup>2</sup> )	0.06	0.10	0.06	0.10
Defrost interval (min)	105.50	104.80	99.10	102.40
Defrost time (min)	5.70	4.80	5.30	4.50
Defrost power (W-H) <sup>a</sup>	210.30	190.00	280.60	244.20
Frost/Defrost COP <sup>b</sup>	2.22	2.27	2.18	2.20

<sup>a</sup> Measured power consumption of compressor and indoor blower.

<sup>b</sup> Integrated average COP includes 5 kW of auxiliary heat during defrost period.

Previous work by Miller<sup>17</sup> indicated that increasing the effective flow area through the indoor throttle, active in defrost mode, would improve defrost efficiency by increasing refrigerant flow during the first few minutes of defrost. The defrost intervals for tests listed in Table 2 are similar, indicating similar frost loads. Roughly doubling the flow area through the indoor throttle caused the defrosting time to decrease 15% and the defrost power to decrease roughly 10% compared to tests with fixed throttle opening. This control resulted in a 2% increase in COP (including 5 kW of auxiliary heat), integrated over the frosting and defrosting cycles. Doubling the throttle flow area and overspeeding the compressor to 90 Hz during defrost caused a 1% drop in integrated average frost/demand defrost COP as compared to defrosting at 60 Hz.

The works of Kuwahara et al.<sup>6</sup> and Itoh<sup>18</sup> indicated improvement in defrosting and system efficiency through compressor overspeeding and control of the throttle flow area during defrosting. Glamm<sup>7</sup> indicated only slight improvement in average frost/demand defrost COP resulting from control of the throttle flow area. The results in Table 2 indicate, for the given configured system, that the best average frost/defrost COP results by increasing the flow area of the indoor throttle and by operating the compressor at 60-Hz drive frequency during defrosting. Further testing also revealed that regardless of compressor drive frequency prior to the defrost cycle, the best average frost/demand defrost COP was observed with the compressor driven at 60 Hz during defrosting.

#### Characterized CVSHP Cycling Dynamics and Improved Cycling Efficiency

The slow response of the test unit at speeds less than 60 Hz caused an increase in the degradation coefficient ( $C_D$ ) for normal mode cycling (i.e., compressor and fans cycle on and off simultaneously), as seen in Table 3. Attempts were made to improve cycling efficiency by initially increasing the area of the throttle at start-up. Heating mode results indicated that the larger flow area only increased the level of refrigerant in the accumulator after start-up (visually observed through sight glasses on the accumulator) and caused a decrease in cycling efficiency. In cooling mode the refrigerant charge was more evenly distributed between the heat exchangers prior to start-up. At start-up the larger flow area through the indoor throttle caused less restriction to the flow and allowed the compressor to more rapidly establish charge distribution. Therefore, by controlling the indoor throttle, the  $C_D$ s measured during low compressor speed operation were improved for normal cooling mode cycling.

**TABLE 3**  
**Degradation coefficients ( $C_D$ ) observed for**  
**various compressor speeds and cycling strategies**

Mode of operation	Compressor speed (Hz)	$C_D$ s for various cycling control strategies				
		Normal		Overspeed 20S <sup>a</sup>	Refrigerant control, blower delay (off-cycle)	
Expansion valve setting		Fixed	Variable	Fixed	Fixed	Variable
Heating	60	0.225			0.113	
	30	0.329	0.391	0.295	0.215	0.133
	15	0.405				
Cooling	60	0.169			0.060	
	30	0.365	0.237			
	15	0.362	0.217	0.209	0.162	0.102

<sup>a</sup>At start-up the compressor is driven at 60 Hz for 20 S.

Cycling control strategies. Heating and cooling mode tests were conducted with the refrigerant isolated in the system high-side during the off-cycle and with the indoor blower continuing to operate for 2 min into the off-cycle. At start-up the throttle was controlled for best cycling efficiency. The results of both heating and cooling mode tests with refrigerant migration and throttle control are displayed in Fig. 10 and are compared to normal mode cycling test results.

Heating mode cycling test results in Fig. 10 reveal significant improvement in efficiency. The tests, conducted at 30-Hz compressor drive frequency, show the CVSHP to achieve near steady state performance in roughly 10 min by controlling the off-cycle refrigerant migration. The  $C_D$  decreased from 0.329 for normal mode cycling

to 0.133 with combined control of off-cycle migration, 2 min of indoor blower delay, and throttle control (Table 3).

Cooling mode cycling test results with refrigerant migration and throttle control observed at 15-Hz compressor drive frequency were not as dramatic as results observed in the heating mode. However, off-cycle control of refrigerant migration did improve the cycling COP of the CVSHP (Fig. 10). The  $C_D$  decreased from 0.362, for normal mode cycling at 15-Hz speed, to 0.102, for cycling with off-cycle migration control, 2-min delay in indoor blower operation, and throttle control (Table 3).

#### Seasonal Performance Analyses for SSHP and CVSHP

Comparisons of seasonal performance simulations were made for the different heat pump configurations listed in Table 4. Steady state COPs of each system were based on the compressor and indoor blower both powered by ideal induction motor drives (i.e., sine-wave driven). A conventional SSHP,<sup>f</sup> having capillary tube flow control and a 90-min time/temperature defrost control, was compared with the optimally controlled CVSHP operating only at 60 Hz drive frequency (i.e., single-speed unit with optimal flow control and reduced dynamic losses).<sup>17</sup> The optimally controlled breadboard CVSHP, having reduced dynamic losses, was then compared with the CVSHP operating only at 60-Hz drive frequency (i.e., optimal control single-speed) to quantify the benefit of modulation on a seasonal

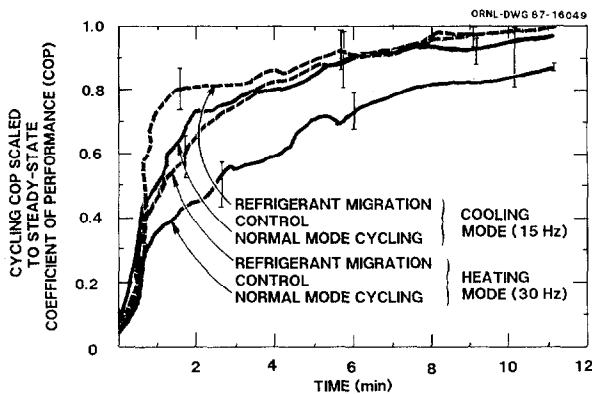


Fig. 10. Improvement in heating and cooling mode cycling COP. Cycling rate 12 min on, 48 min off.

<sup>f</sup> Actually the original unmodified CVSHP operated with the compressor driven by 60-Hz sine wave.

**TABLE 4**  
**Heat Pump Systems used in APF Comparisons,**  
**Compressor and Fans Sine-Wave Driven**

Heat Pump System	Refrigerant Flow Control	Indoor Airflow	Cycling $C_D$		Defrost Control	COP <sup>a</sup> Heat	EER <sup>b</sup> Cool
			Heat	Cool			
Conventional Single-Speed	Capillary	Constant	0.25	0.18	90-min Time & Temperature	3.0	8.70
Optimal Control Single-Speed	Variable Area	Constant	0.11	0.06	Demand	3.1	9.66
CVSHP	Variable Area	Variable	0.13	0.10	Demand	3.1	9.66

<sup>a</sup>Heating COP measured at 47 F (8.3°C) outdoor air temperature (60-Hz compressor drive frequency).

<sup>b</sup>Cooling EER measured at ARI rating point of 80 F (27°C) DB/67 F (19°C) WB indoor and 82 F (28°C) outdoor temperature (60-Hz compressor drive frequency).

basis for the particular system tested. For the seasonal simulations the CVSHP modulation ratio was 3:1 (90- to 30-Hz compressor speed) in heating mode and 4:1 (60- to 15-Hz compressor speed) in cooling mode.

Total annual energy use due to frosting/defrosting, cycling, and supplemental heat was calculated for the heat pump systems (Table 4), operating in Fort Worth, Knoxville, and Syracuse. Energy use for each of the loss categories along with steady state and total annual operating energy use are listed in Table 5.

SSHP reduced dynamic losses. Only 1% of annual energy consumption was attributable to frosting. Demand defrost control as compared to a 90-min time-temperature defrost control reduced the number of seasonal defrosts by roughly a factor of 3 for all three locations. Both demand defrost control and improvement in defrost efficiency<sup>g</sup> caused the frosting/defrosting energy consumptions for an optimally controlled SSHP to be roughly half that observed for an SSHP, having fixed throttle and time-temperature defrost control.

The combined control of off-cycle refrigerant migration and delay in shutdown of the indoor blower substantially reduced cycling losses for the optimally controlled SSHP by roughly

<sup>g</sup> Throttle fully open during defrost to increase refrigerant circulation for improved defrost efficiency.

50% for simulated operation in Fort Worth, Knoxville, and Syracuse (Table 5).

CVSHP modulation effect. The added feature of continuous modulation of the compressor and indoor blower motors further improved system efficiency significantly as seen by the reduction of energy consumption (Table 5). This improvement in system efficiency can be attributed to (1) reduced supplemental heat, (2) reduced cycling losses, (3) heat exchanger unloading, and (4) reduced frosting/defrosting losses as explained in the following paragraphs.

Reduced supplemental heat. Overspeeding the compressor reduced the balance point of the CVSHP as compared with the optimally controlled SSHP and reduced the amount of supplemental heat required to match load (i.e., balance points listed in Table 5). In the more severe winter climate of Syracuse the CVSHP reduced supplemental heat usage by 43%. The compressor overspeeding capability would also reduce the peak power demand for the public utility company.

Reduced cycling losses. For operation at ambient temperatures greater than the balance point, the better load following capability of the CVSHP reduced cycling losses simply by reducing the number of cycles. Assuming both configured heat pumps to have reduced dynamic losses, compressor and indoor blower speed modulation decreased cycling energy consumption roughly by 40% of cycling energy for the optimally controlled SSHP.

**TABLE 5**  
**Simulated annual energy use breakdown for single-speed heat pump**  
**and continuously variable speed heat pumps**

City and state	Heat pump configuration	Heating balance point [F (°C)]	Annual back-up heat <sup>a</sup> (kWh)	Dynamic loss energy		Steady-state energy (kWh)	Total annual energy <sup>d</sup> (kWh)	Yearly defrosts	Annual performance factor (APF)
				Fr/Def <sup>b</sup> (kWh)	Cycling <sup>c</sup> (kWh)				
Ft. Worth, Tex.	Conventional single-speed	21.0 (-6.1)	94.5	437.3	1257.7	9032.4	10822.0	519	2.13
	Optimal control single-speed	21.0 (-6.1)	91.6	140.7	549.0	8332.6	9114.0	139	2.52
	CVSHP	17.5 (-8.1)	30.3	97.2	293.0	6742.3	7162.8	105	3.21
Knoxville, Tenn.	Conventional single-speed	22.0 (-5.6)	234.7	784.1	1278.5	7502.2	9799.4	911	2.03
	Optimal control single-speed	22.0 (-5.6)	244.9	338.0	594.7	6815.0	7992.6	304	2.49
	CVSHP	18.0 (-7.8)	94.1	225.7	345.0	5618.3	6283.2	236	3.16
Syracuse, N.Y.	Conventional single-speed	27.0 (-2.8)	3073.2	1994.7	1156.3	10232.3	16456.5	2008	1.73
	Optimal control single-speed	27.0 (-2.8)	3178.1	1192.8	545.4	9555.2	14471.6	855	1.97
	CVSHP	21.0 (-6.1)	1806.3	950.8	321.0	9344.0	12422.2	847	2.30

<sup>a</sup> Auxiliary heat required to satisfy house heating load when heat pump operates below balance point. Does not include auxiliary heat (5 kW) attributed to defrost.

<sup>b</sup> Frosting/defrosting includes recovery energy following defrost and 5 kW of auxiliary heat during reverse-cycle defrost.

<sup>c</sup> Cycling includes off-cycle parasitics.

<sup>d</sup> Heat pump yearly energy consumption including back-up heat.

*Heat exchanger unloading.* Modulating the CVSHP at low loads reduced the condensing and raised the evaporating pressure (heat exchanger unloading) and thereby improved steady state COP as previously observed by Miller.<sup>9</sup> This heat exchanger unloading yielded the largest reduction in heat pump energy usage for Fort Worth and Knoxville. The steady state energy consumption of the CVSHP was reduced by 19% compared with the optimally controlled SSHP in Fort Worth. In Knoxville, the steady state usage was reduced by 17.5%, and in Syracuse, by only 2%. The small reduction in Syracuse probably occurred because the majority of load hours occurred at nominal compressor speed (i.e., 60-Hz drive frequency) in this predominantly heating load climate.

*Reduced frosting/demand defrosting losses.* The frosting/demand defrosting efficiency of the CVSHP improved slightly over that of the optimally controlled SSHP. A maximum decrease in frost/demand defrost energy consumption of 30% was observed for the CVSHP in Knoxville as compared with the optimally controlled SSHP. The number of simulated defrosts in Knoxville for the CVSHP was 236 as compared with 304 defrosts for the SSHP. During low-speed modulation the evaporator temperature increased and therefore the defrost interval increased resulting in the reduced number of seasonal defrosts. In Syracuse the number of defrosts were nearly equal, again probably because the majority of heating load hours occurred at nominal compressor speed (i.e., 60-Hz drive frequency).

#### Benefits of the CVSHP

The seasonal analysis results for simulated operation in Syracuse showed that a CVSHP improved annual performance factor (APF) 16% compared to an optimally controlled SSHP. The test CVSHP operating in Knoxville or Fort Worth would improve APF roughly 27%. The major improvement in seasonal efficiency in the moderate climates resulted from the ability to unload the heat exchangers during low load operation. In the predominantly heating load climate of Syracuse, the major improvement resulted from the reduction of supplemental heat usage. The CVSHP reduces dynamic losses roughly 50 to 70% of dynamic losses observed for the optimally controlled SSHP.

CVSHPs offer other benefits that are not easily quantifiable. In the heating season the CVSHP can reduce utility peak demand by overspeeding the compressor. In the cooling mode the CVSHP's near constant operation would help improve humidity control as compared to an SSHP. Also the fewer number of on/off and defrost cycles would improve compressor reliability.

Finally, the CVSHP could be used for zone control by adjusting capacity appropriately for the zoned load.

#### Future Activities

A compressor calorimeter, having a capacity range of 6 to 50 kBtus, is currently being installed for the testing of variable speed compressors. The test facility will provide the capability to generate a more complete data base for state-of-the-art variable speed compressors as described further by Rice,<sup>2</sup> and will allow improvement of present modulating compressor submodels for the ORNL modulating heat pump analytical design tool package. Modulating scroll and rotary compressors are planned to be tested during the upcoming year. Compressor testing may also be conducted with alternative refrigerants that could substitute for fully halogenated CFC refrigerants.

A request for proposal is being issued for experimental evaluation of the performance of state-of-the-art variable speed Japanese heat pumps. Tests will be conducted to characterize the system performance under steady state, cycling, and frosting/defrosting conditions.

#### References

1. W. A. Miller, *Laboratory Study of the Dynamic Losses of a Single-Speed, Split System Air-to-Air Heat Pump Having Tube and Plate Fin Heat Exchangers*, ORNL/CON-253, Oak Ridge National Laboratory, Oak Ridge, Tenn. (to be published).
2. C.K. Rice, "Capacity Modulation Component Characterization and Design Tool Development," *Proc. of the ORNL/DOE Heat Pump Conference*, April 17-20, 1988.
3. D.G. Erbs, C.E. Bullock, and R.J. Voorhis, "New Testing and Rating Procedures for Seasonal Performance of Heat Pumps with Variable Speed Compressors," *ASHRAE Trans.*, 92 (Pt. 2), 1986.
4. N. Tanaka and G. Yamanaka, "Experimental Study on the Dynamic Characteristics of a Heat Pump," *ASHRAE Trans.*, 88 (Pt. 2) (1982).
5. W. A. Miller, "The Laboratory Evaluation of the Heating Mode Part-Load Operation of an Air-to-Air Heat Pump," *ASHRAE Trans.*, 91 (Pt. 2B) (1985).
6. E. Kuwahara, T. Kawamura, and M. Yamazaki, "Shortening the Defrost Time on a Heat-Pump

- Air Conditioner," *ASHRAE Trans.*, 92 (Pt. 2A) (1986).
7. P. Glamm, *Dynamic Control of Heat Pumps*, EPRI EM-5082, Electric Power Research Institute, Palo Alto, Calif., Project 2033-11.
  8. C. K. Rice, S. K. Fischer, and C. J. Emerson, *The Oak Ridge Heat Pump Models: II. An annual performance factor/loads model for residential air-source heat pumps*, ORNL/CON-160, Oak Ridge National Laboratory, Oak Ridge, Tenn., to be published.
  9. W. A. Miller, "Steady State Refrigerant Flow and Airflow Control Experiments Conducted on a Continuously Variable Speed Air-to-Air Heat Pumps," *ASHRAE Trans.*, 93 (Pt. 2) (1987).
  10. S. K. Fischer and C. K. Rice, *The Oak Ridge Heat Pump Models: I. A Steady-State Computer Design Model for Air-to-Air Heat Pumps*, ORNL/CON-80/R1, Oak Ridge National Laboratory, Oak Ridge, Tenn., August, 1983.
  11. E. A. Skogsholm, "Efficiency and Power Factor for a Square Wave Inverter Drive," *IEE-IAS*, October 1978.
  12. N. Mohan, *Techniques for Energy Conservation in AC Motor-Driven Systems*, EPRI EM-2037, Electric Power Research Institute, Palo Alto, Calif., 1981.
  13. J. C. Andreas, *Energy-Efficient Electric Motors*, Marcel Dekker, Inc., New York, 1982.
  14. J. J. Jacobs, "Analytical and Experimental Techniques for Evaluating Compressor Performance Losses," *Proceedings of the 1976 Purdue Compressor Technology Conference*, West Lafayette, Indiana, July 1976.
  15. J. D. Lloyd, "Variable-Speed Compressor Motors Operating on Inverters," *ASHRAE Trans.*, 88 (Pt. 1) (1982).
  16. C. K. Rice, "Efficiency Characteristics of Speed Modulated Drives at Predicted Torque Conditions for Air-to-Air Heat Pumps," *ASHRAE Trans.*, 84 (Pt. 1) (1988).
  17. W. A. Miller, "Laboratory Examination and Seasonal Analysis of Frosting and Defrosting for an Air-to-Air Heat Pump," *ASHRAE Trans.*, 93 (Pt. 1) (1987).
  18. H. Itoh, "Improvement of a Heat Pump Room Air-Conditioner by Use of Pulse-Motor-Driven Expansion Valve," *ASHRAE Trans.*, 92 (Pt. 92) (1986).



CONF-8804100

**Proceedings of the  
2nd DOE/ORNL Heat Pump Conference:  
Research and Development on Heat Pumps  
for Space Conditioning Applications**

Crystal Gateway Marriott  
Washington, D.C.  
April 17-20, 1988

Published: August 1988

Prepared by the  
Oak Ridge National Laboratory  
Oak Ridge, Tennessee 37831  
operated by  
Martin Marietta Energy Systems, Inc.  
for the  
U.S. DEPARTMENT OF ENERGY



# Contents

Foreword .....	v
<b>Session 1. Electric Heat Pump Technology: Current Activities</b>	
Advanced Refrigeration Systems Program Overview	
<i>T. G. Statt</i> .....	3
Laboratory Capacity Modulation Experiments, Analyses, and Validation	
<i>W. A. Miller</i> .....	7
Capacity Modulation Component Characterization and Design Tool Development	
<i>C. K. Rice</i> .....	23
Evaluation of Vapor Compression Cycles Using Nonazeotropic Refrigerant Mixtures	
<i>R. L. Merriam</i> .....	35
Evaluation of Nonazeotropic Refrigerant Mixtures for Capacity Modulation	
<i>E. A. Vineyard and J. R. Sand</i> .....	47
Experimental Evaluation of Two Refrigerant Mixtures in a Breadboard Air Conditioner	
<i>W. Mulroy, M. Kauffeld, M. McLinden, and D. A. Didion</i> .....	55
<b>Session 2. Electric Heat Pump Technology: Related Research</b>	
Heat Pump Research at the Electric Power Research Institute	
<i>A. Lannus</i> .....	65
Overview of Ground-Coupled Heat Pump Research and Technology Transfer Activities	
<i>V. D. Baxter and V. C. Mei</i> .....	75
<b>Session 3. What Should Influence the Future Direction of the DOE/ORNL R&amp;D Program?</b>	
Assessment of Japanese Variable-Speed Heat Pump Technology	
<i>Kenji Ushimaru</i> .....	85
CFC Restrictions: Energy Impacts and Technological Alternatives	
<i>F. A. Creswick and S. K. Fischer</i> .....	93
International Cooperation in Heat Pump and Refrigeration Research Through the International Energy Agency	
<i>J. D. Ryan</i> .....	101
<b>Session 4. Thermally Activated Heat Pumps: Absorption Systems</b>	
DOE Absorption Program Overview	
<i>R. C. DeVault</i> .....	105
Development of an Advanced-Cycle Absorption Heat Pump for Residential Applications	
<i>B. A. Phillips</i> .....	111
Evaluation of a Commercial Advanced Absorption Heat Pump Breadboard	
<i>R. J. Modahl and F. C. Hayes</i> .....	117
Development and Proof-Testing of Advanced Absorption Refrigeration-Cycle Concepts — Phase II	
<i>R. C. Reimann and Gorken Melikian</i> .....	127

Absorption Enhancement Research and Related Diagnostics <i>H. Perez-Blanco, M. R. Patterson, D. T. Bostick, and L. N. Klatt</i> .....	133
Worldwide Survey of Absorption Fluids Data <i>R. A. Macriss and T. S. Zawacki</i> .....	145

### Session 5. Heat-Actuated Heat Pumps: Engine-Driven Heat Pumps

GRI Heat Pump R&D Program Overview <i>A. R. Maret</i> .....	153
Engine-Driven Heat Pump Program Overview <i>G. T. Privon and A. T. Braun</i> .....	155
Status of the Braun Engine-Driven Heat Pump Development <i>A. T. Braun, R. J. Prekker, and A. P. Schneeberger</i> .....	161
An Analytical Study of Hybrid Ejector/Internal Combustion Engine-Driven Heat Pumps <i>R. W. Murphy</i> .....	163
Entrainment Enhancement of a Supersonic Jet for Advanced Ejectors <i>W-H. Jou, G. S. Knoke, and C-M. Ho</i> .....	169

### Session 6. Thermally Activated Heat Pumps: Stirling Engine-Driven Heat Pumps

An Overview of the Stirling Engine Heat Pump Program <i>F. C. Chen</i> .....	177
Development of a Residential Free-Piston Stirling Engine Heat Pump <i>R. A. Ackermann</i> .....	189
Preliminary Assessment of a Magnetically Coupled Free-Piston Stirling Engine Heat Pump Compressor <i>W. T. Beale and G. Chen</i> .....	197
Integration of Analysis and Experiment for Stirling Cycle Processes. Part 1: Gas Spring Hysteresis Loss <i>A. A. Kornhauser and J. L. Smith, Jr.</i> .....	203
Comparative Assessment of Free-Piston and Kinematic Stirling Engine Technologies <i>W. P. Teagan</i> .....	209
Author Index .....	211
Conference Attendees .....	213
Appendix A .....	221